Thermodynamics and correlations of a helical spin chain with non-magnetic impurities

1990 J. Phys.: Condens. Matter 2 953

(http://iopscience.iop.org/0953-8984/2/4/015)

J. Phys.: Condens. Matter **2** (1990) 953–967. Printed in the UK

Thermodynamics and correlations of a helical spin chain with non-magnetic impurities

I Harada† and H J Mikeska
Institut für Theoretische Physik, Universität Hannover, Appelstrasse 2, 3000 Hannover 1, Federal Republic of Germany

Received 30 August 1988, in final form 21 August 1989

Abstract. The effect of non-magnetic impurities on the thermodynamics of a classical helimagnetic chain with antiferromagnetic nearest-neighbour and next-nearest-neighbour interactions is studied by means of the transfer matrix method. The results for the partition function and the nearest-neighbour and the next-nearest-neighbour spin correlation functions are obtained exactly for both the isotropic Heisenberg model and the planar model as functions of temperature and concentration of non-magnetic impurities. The magnetic susceptibility is calculated up to terms linear in the concentration. It is found that a non-magnetic impurity modifies the helical spin structure in its vicinity and leads consequently to the formation of a new local equilibrium spin structure, which is called a spin complex. The consequences of this peculiar spin complex on the thermodynamics, especially on the spin-correlation functions, are extensively discussed in connection with experimental results on $FeMgBO_4$.

1. Introduction

A non-magnetic impurity plays a crucial role in a one-dimensional spin chain. This is obvious in the case where only nearest-neighbour (NN) interactions exist, because the path of spin correlation cannot avoid a non-magnetic impurity site, at which a magnetic chain is completely broken up. This effect causes, for example, the novel phenomenon of the crossover of anisotropic susceptibilities (Harada *et al* 1980) as well as the strong reduction in the Néel temperature in quasi-one-dimensional magnetic systems (Hone *et al* 1975). On the other hand, when the system includes next-nearest-neighbour (NNN) interactions the situation is rather different and is less clear than in the former case (Villain 1979).

Let us envisage the effect of a single non-magnetic impurity on the ground-state spin structure of a magnetic chain in the following two situations:

(i) The ground state of the host is antiferromagnetic.
(ii) The ground state of the host has the helical spin structure.

Case (i) occurs when the ratio between the NN interaction constant $2J_1$ and the NNN interaction constant $2J_2$ (both are assumed to be antiferromagnetic in this paper), i.e. $j = J_2/J_1$, is smaller than 0.25. In this case the antiferromagnetic spin structure persists

† Present address: Department of Physics, Faculty of Science, Kobe University, Rokkodai, Kobe 657, Japan.

0953-8984/90/040953 + 15 $03.50

even when the system is diluted, although the sublattices are interchanged at the impurity site because one spin is missing there. On the other hand, when the ratio j is greater than 0.25, the helical spin structure occurs. It is conceivable that, in this spin structure, a non-magnetic impurity modifies the helical spin structure and leads consequently to a new local equilibrium spin structure. We call it a spin complex in this paper. The spin structure of this spin complex is not obvious (Harada and Mikeska 1988b).

Thus the purpose of this paper is to study the effect of non-magnetic impurities on the thermodynamics of the helical spin chain described by the following Hamiltonian:

$$H = 2J_1 \sum_{p=1}^{N-1} \boldsymbol{S}_p \cdot \boldsymbol{S}_{p+1} + 2J_2 \sum_{p=1}^{N-2} \boldsymbol{S}_p \cdot \boldsymbol{S}_{p+2} \tag{1}$$

where $\boldsymbol{S}_p$ denotes a unit vector at site p, $\boldsymbol{S}_p = (\sin\Theta_p \cos\Phi_p, \sin\Theta_p \sin\Phi_p, \cos\Theta_p)$ for the Heisenberg model or $\boldsymbol{S}_p = (\cos\theta_p, \sin\theta_p)$ for the planar model. We assume that the chain has N sites with free ends. We here note that the spin magnitude factor $\sqrt{S(S+1)}$ is absorbed in the exchange interaction constants. In this paper, the previous theory of the transfer matrix method for the pure systems (Harada 1984, Harada and Mikeska 1988a) will be extended to include non-magnetic impurities. Exact results for the internal energy, the specific heat, the NN spin correlation function and the NNN spin correlation function for an arbitrary concentration of non-magnetic impurities will be presented. The susceptibility will be calculated up to terms linear in the concentration.

It is worthwhile noticing that the material $FeMgBO_4$ may be described by our model. Here magnetic Fe^{3+} ions form a zigzag chain in the c direction with distances of 2.9 Å between NNs and 3.1 Å between NNNs (Weidenmann 1979). Thus, the NN interaction $2J_1$ and the NNN interaction $2J_2$ inside the chains are of the same order of magnitude. Furthermore, there exists a crystallographic site inversion of about 15% between magnetic Fe^{3+} ions and non-magnetic Mg^{2+} ions and this fact makes this material a diluted system (Wiedenmann 1979). In fact, Weidenmann *et al* (1983) and Weidenmann and Mezei (1986) found in this material not only characteristics of a helimagnet but also magnetic behaviour of spin-glass type. We are interested in experimental data, in particular, on the correlation functions. The sum of NN and NNN correlation functions exhibits a saturation tendency at low temperatures (Weidenmann *et al* 1981). We try to interpret this behaviour as a result of the spin complex mentioned above. In addition, the observed susceptibility shows a broad maximum at a certain temperature, which is very low compared with that in ordinary NN antiferromagnets (Weidenmann and Burlet 1978). We shall demonstrate that this fact is also consistent with our numerical results.

In the next section, we formulate the transfer matrix method appropriate for a diluted Heisenberg model with NN and NNN interactions and obtain the thermodynamic quantities in terms of the eigenvalues and the eigenfunctions of the integral equations for the pure systems. In § 3, we treat the planar model in a similar way as in the Heisenberg model. Numerical results for both models are presented and discussed in § 4. The last section (§ 5) is devoted to the conclusion.

2. Isotropic Heisenberg chain

2.1. Partition function and free energy

Let us first recall the procedure for obtaining the exact partition function in the pure case (Harada and Mikeska 1988a). The partition function for the pure Heisenberg spin chain with n spins is given by

$$Z_n = \left(\prod_{p=1}^{n} \int \mathrm{d}\Omega_p\right) \exp\left[-\left(\sum_{p=1}^{n-1} \boldsymbol{S}_p \cdot \boldsymbol{S}_{p+1} + j \sum_{p=1}^{n-2} \boldsymbol{S}_p \cdot \boldsymbol{S}_{p+2}\right)\Big/ t\right] \tag{2}$$

where $\mathrm{d}\Omega_p$ denotes the volume element of the solid angle for $\boldsymbol{S}_p$ and $t = k_B T/2J_1$, k_B being the Boltzmann constant and T denoting absolute temperature. The multiple integration in equation (2) can conveniently be carried out iteratively. Integrate first over $\boldsymbol{S}_1$ for a *given* configuration of $\boldsymbol{S}_2, \boldsymbol{S}_3, \ldots \boldsymbol{S}_n$. Describing $\boldsymbol{S}_1$ in polar coordinates with $\boldsymbol{S}_2$ as the polar axis and with an arbitrary direction in the plane perpendicular to $\boldsymbol{S}_2$ to define the zero of the azimuthal angle Φ_1, the result of this integration depends only on the angle between $\boldsymbol{S}_2$ and $\boldsymbol{S}_3$. Therefore we can iterate the procedure, integrating over $\boldsymbol{S}_2$ for a *given* configuration of $\boldsymbol{S}_3, \ldots, \boldsymbol{S}_n$ and continuing the iteration to work through the chain. This gives the result

$$Z_n = \left(\prod_{p=1}^{n} \int 2\,\mathrm{d}\Omega_p\right) \exp\left(\frac{-(\cos\Theta_1 + \cos\Theta_{n-1})}{2t}\right) \prod_{p=1}^{n-2} A(\Theta_p, \Theta_{p+1}; \Phi_p) \tag{3}$$

where

$$A(\Theta_p, \Theta_{p+1}; \Phi_p) = \tfrac{1}{2} \exp[-(\cos\Theta_p + \cos\Theta_{p+1})/2t - j(\cos\Theta_p \cos\Theta_{p+1} + \sin\Theta_p \sin\Theta_{p+1} \cos\Phi_p)/t]. \tag{4}$$

This result is the appropriate generalisation of the result for the isotropic NN Heisenberg chain as given by Fisher (1964). For NN interactions the polar axis is defined as above by the neighbouring spin but the integrand does not depend on the azimuthal angle Φ, and the integral is a constant; for NNN interactions the integrand does depend on Φ, the integral over $\boldsymbol{S}_p$ depends on $x_{p+1} = \cos\Theta_{p+1}$ and the iterative integration leads to the convolution structure of equation (3).

The partition function from equation (3) is equivalent to the partition function of the spin system described by the following Hamiltonian:

$$H^D = \sum_p (2J_2 \boldsymbol{S}_p \cdot \boldsymbol{S}_{p+1} + 2J_1 S_p^z). \tag{5}$$

We thus find that the statistical mechanics of the isotropic Heisenberg model with NN and NNN interactions are governed by the same integral equation as the NN model in an external magnetic field (Blume *et al* 1975). In analogy to the planar model (Harada 1984) the Heisenberg chain in an external magnetic field is called the dual model for the system defined in equation (1). The situation is illustrated schematically in figure 1(*a*). Owing to the non-commutativity of rotations in three dimensions this duality, in contrast to the corresponding property of the planar model, cannot be derived on the level of the Hamiltonian but only on the basis of an explicit comparison of the transfer integral calculations for the two models.

We now proceed to the evaluation of the partition function as given in equation (3). Since the integrations over $\{\Phi_p\}$ are separable, they result in the zeroth-order modified Bessel function. The kth-order Bessel function is defined by the integral

$$I_k(z) = \frac{1}{2\pi} \int_{-\pi}^{\pi} \mathrm{d}\Phi \exp(z \cos\Phi) \cos(k\Phi). \tag{6}$$

On the other hand, to perform the multiple integration over $\{\Theta_p\}$ we introduce the following integral equation (Blume *et al* 1975):

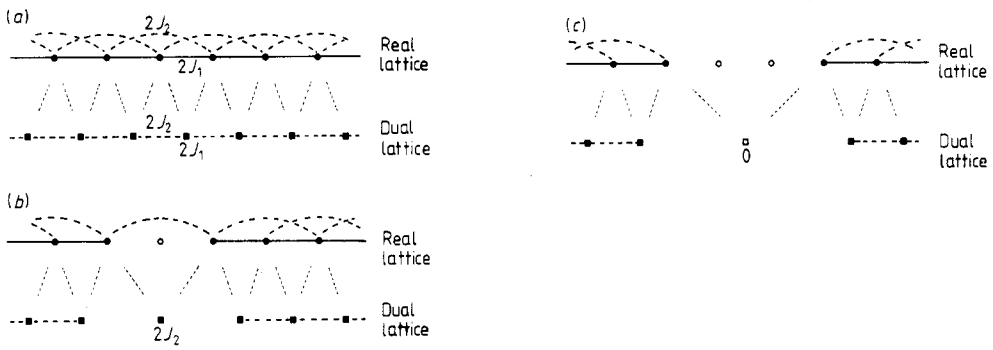

Figure 1. The correspondence between a real lattice and a dual lattice; (*a*) the pure case; (*b*) the magnetic chain involving a single non-magnetic impurity; (*c*) the magnetic chain involving two non-magnetic impurities which occupy the NN sites. In the real lattice, each full line and each broken line represent, respectively, the NN interaction constant $2J_1$ and the NNN interaction constant $2J_2$ between spins denoted by the full circles. An open circle represents a non-magnetic impurity. In the dual lattice, on the other hand, spins denoted by the full squares couple to the NN spins with interaction constant $2J_2$ and are in an applied field of magnitude $2J_1$. The spin at the centre of (*b*) is an impurity spin isolated from others but in an applied field of magnitude $2J_2$ while that of (*c*) is an isolated impurity spin in a zero field.

$$\int_{-1}^{1} \mathrm{d}x_2\, A_0(x_1, x_2)\psi_m(x_2) = \lambda_m \psi_m(x_1) \tag{7}$$

where

$$A_k(x_1, x_2) = \exp[-(x_1 + x_2)/2t - jx_1x_2/t]\, I_k\{-j[(1 - x_1^2)(1 - x_2^2)]^{1/2}/t\} \tag{8}$$

Here we have changed integral variables from $\{\cos \Theta_p\}$ to $\{x_p\}$. We solve this integral equation by means of the Gaussian quadrature (Blume *et al* 1975). Utilising the well known expansion of the kernel A_0 with respect to λ_m and ψ_m and employing the orthonormality relation among ψ_m, we obtain Z_n:

$$Z_n = \sum_m B_m^2 \lambda_m^{n-2} \tag{9}$$

where

$$B_m = \int_{-1}^{1} \mathrm{d}x \exp\left(-\frac{x}{2t}\right)\psi_m(x) \tag{10}$$

is the quantity characterising free-end effects. When $n \to \infty$, Z_n is dominated by the largest eigenvalue λ_0 and the eigenfunction ψ_0 belonging to λ_0.

Now, we consider a diluted system with Nx non-magnetic impurities, x being the concentration of non-magnetic impurities. As is shown in figure 1(*b*), a single non-magnetic impurity does not break up the chain and the spins on both sides of the impurity are still coupled by the NNN interaction without competition. This corresponds in the dual lattice to the isolated impurity spin in a field $2J_2$. Two or more consecutive non-magnetic impurities break up a chain completely at these sites, as is seen in figure 1(*c*). This corresponds in the dual lattice to the existence of an isolated spin free from a field. Thus, the addition of non-magnetic impurities leads to break-up of the dual lattice into isolated impurity spins and isolated chain segments of finite lengths.

From these observations we realise the important consequence that, when non-magnetic impurities are introduced, all information carried by the transfer matrix is lost at the impurity sites (which correspond to free ends in the dual lattice). This fact enables us to calculate the partition function as a product of the partition functions for the independent segments having finite lengths with n spins. Since the density (per site) of segments with n spins is given by

$$P_n(x) = x^2(1-x)^n \tag{11}$$

which is normalised as

$$\sum_{n=1} [nP_n(x) + nP_n(1-x)] = 1 \tag{12}$$

the partition function of the diluted system is given by

$$Z_N = Z_0^{NP_1(1-x)} \prod_{n=2} Z_n^{NP_n(x)}. \tag{13}$$

Here Z_n is the partition function for the finite chain with n spins and is given by equation (9) while Z_0 is the contribution from NNN spins next to an impurity and is given by $L_0(-j/t)$, where $L_k(z)$ is defined by

$$L_k(z) = \tfrac{1}{2}\int_{-1}^{1} \mathrm{d}x\, x^k \exp(zx). \tag{14}$$

As a result, we obtain the following dimensionless free energy per site:

$$\begin{aligned} f &= (\ln Z_N)/N \\ &= (1-x)^3(\ln \lambda_0 + x \ln B_0^2) + x(1-x)^2\left\{\ln\left[L_0\left(-\frac{j}{t}\right)\right] + x \ln\left[L_0\left(-\frac{1}{t}\right)\right]\right\} \\ &\quad + \sum_{n=1} x^2(1-x)^{n+2} \ln\left[\sum_m \left(\frac{B_m}{B_0}\right)^2 \left(\frac{\lambda_m}{\lambda_0}\right)^n\right]. \end{aligned} \tag{15}$$

The internal energy ε in units of $2J_1$ and the specific heat C in units of k_B are obtained using the following formulae:

$$\varepsilon = t^2 \partial f/\partial t \tag{16}$$

$$C = \partial \varepsilon/\partial t. \tag{17}$$

2.2. *Correlation function and susceptibility*

A correlation function $W_r = \langle \boldsymbol{S}_p \cdot \boldsymbol{S}_{p+r} \rangle$ for the diluted system is an average over all configurations of non-magnetic impurities. First we consider the NN correlation function $W_1 = \langle \cos \Theta_p \rangle$, which corresponds to the magnetisation in the dual lattice. The magnetisation at a certain site depends only on the distances from the nearest non-magnetic impurities on both sides. The configurations of non-magnetic impurities other than these two non-magnetic impurities do not affect the magnetisation at the site. In other words,

it depends only on the length of the segment and on its location within the segment. Then, we can carry out the calculation for W_1 exactly, obtaining

$$W_1 = \sum_{n=2} P_n(x) W_1(n) \tag{18}$$

where $W_1(n)$ is the NN correlation function summed over all configurations within a finite chain with n (≥ 2) spins:

$$W_1(n) = \frac{1}{Z_n} \sum_k \sum_m B_k B^x_{km} B_m \sum_{q=0}^{n-2} \lambda_m^q \lambda_k^{n-2-q}$$

$$= \frac{1}{Z_n} \sum_k \sum_m B_k B^x_{km} B_m \frac{\lambda_k^{n-1} - \lambda_m^{n-1}}{\lambda_k - \lambda_m}. \tag{19}$$

Here we have defined the following integration:

$$B^x_{km} = \int_{-1}^{1} \mathrm{d}x\, \psi_k(x) x \psi_m(x). \tag{20}$$

By inspection, we see that $W_2 = \langle \cos\Theta_p \cos\Theta_{p+1} + \sin\Theta_p \sin\Theta_{p+1} \cos\Phi_p \rangle$ can be calculated exactly in the similar way as

$$W_2 = \sum_{n=3} P_n(x) W_2(n) + x(1-x)^2 \frac{L_1(-j/t)}{L_0(-j/t)} \tag{21}$$

where the second term is the contribution from the NNN spins located just to the right and left of a non-magnetic impurity. The NNN correlation function summed over all configurations within a finite chain with n (≥ 3) spins is given by

$$W_2(n) = \frac{1}{Z_n} \sum_k \sum_g B_k B^{xy}_{kg} B_g \sum_{q=0}^{n-3} \lambda_g^q \lambda_k^{n-3-q}$$

$$= \frac{1}{Z_n} \sum_k \sum_g B_k B^{xy}_{kg} B_g \frac{\lambda_k^{n-2} - \lambda_g^{n-2}}{\lambda_k - \lambda_g} \tag{22}$$

where

$$B^{xy}_{kg} = \sum_m \lambda_m \Bigg(B^x_{km} B^x_{mg} + \int\int_{-1}^{1} \mathrm{d}x_1\, \mathrm{d}x_2\, \psi_k(x_1) \psi_m(x_1) \psi_m(x_2) \psi_g(x_2)$$

$$\times [(1-x_1^2)(1-x_2^2)]^{1/2} \frac{I_1\{-j[(1-x_1^2)(1-x_2^2)]^{1/2}/t\}}{I_0\{-j[(1-x_1^2)(1-x_2^2)]^{1/2}/t\}} \Bigg). \tag{23}$$

The results obtained so far are exact for an arbitrary concentration of non-magnetic impurities. However, calculations of W_r for $r \geq 3$ are not restricted to a segment but depend on the configurations of non-magnetic impurities other than the nearest non-magnetic impurities. Since we know only the information that the finite chain with n spins is formed for a given value of x, we cannot follow the procedure as before. We try to obtain it in the low-concentration limit of non-magnetic impurities. It is easy to show

that the spin correlation function is formally written as a function of the concentration x as

$$W_r = (1-x)^N W_r^{\mathrm{p}} + x(1-x)^{N-1} \sum_h W_r^1(h) + \ldots$$
$$= W_r^{\mathrm{p}} + x\left(-2W_r^{\mathrm{p}} + \sum_h [W_r^1(h) - W_r^{\mathrm{p}})]\right) + \mathrm{O}(x^2) \tag{24}$$

where W_r^{p} denotes the correlation function for a pure system, while $W_r^1(h)$ denotes the correlation function in the chain involving a single non-magnetic impurity at a site h. The sum runs over $N-2$ sites except two sites of the correlating spins.

The correlation function W_r^{p} involves the multiple integral including the matrices, which leads to the rotation of polar coordinates $\{\Theta_q, \Phi_q\}$. By virtue of the block-diagonal form of the matrices after integrations over $\{\Phi_q\}$, the resultant matrices in the integrations over $\{\Theta_q\}$ are 2×2. Thus, we need to solve the following matrix integral equations (Harada and Mikeska 1988a):

$$\int_{-1}^{1} \mathrm{d}x_2\, \mathbf{H}(x_1, x_2)\boldsymbol{u}_m(x_2) = \eta_m \boldsymbol{u}_m(x_1) \tag{25}$$

$$\int_{-1}^{1} \mathrm{d}x_2\, \mathbf{H}^{\mathrm{T}}(x_1, x_2)\boldsymbol{v}_m(x_2) = \eta_m \boldsymbol{v}_m(x_1) \tag{26}$$

where

$$\mathbf{H}(x_1, x_2) = \tfrac{1}{2}\begin{pmatrix} (1+x_1)^{1/2} & (1-x_1)^{1/2} \\ -(1-x_1)^{1/2} & (1+x_1)^{1/2} \end{pmatrix}$$
$$\times \begin{pmatrix} -A_1(x_1, x_2) & 0 \\ 0 & A_0(x_1, x_2) \end{pmatrix} \begin{pmatrix} (1+x_2)^{1/2} & (1-x_2)^{1/2} \\ -(1-x_2)^{1/2} & (1+x_2)^{1/2} \end{pmatrix}. \tag{27}$$

Here $\mathbf{H}^{\mathrm{T}}$ denotes the transposed matrix of $\mathbf{H}$, $\boldsymbol{u}_m$ is a vector with two components u_m^1 and u_m^2, and $\boldsymbol{v}_m$ is a vector with two components v_m^1 and v_m^2. In terms of the eigenvalues and the eigenfunctions, W_r^{p} is written as

$$W_r^{\mathrm{p}} = \sum_m E_{Om} F_{Om} y_m^{r-1} \tag{28}$$

where

$$y_m = \eta_m / \lambda_0 \tag{29}$$

$$E_{km} = \int_{-1}^{1} \mathrm{d}x\, \psi_k(x) U_m(x) \tag{30}$$

$$F_{km} = \int_{-1}^{1} \mathrm{d}x\, \psi_k(x) V_m(x) \tag{31}$$

with

$$U_m = -u_m^1(x)[(1-x)/2]^{1/2} + u_m^2(x)[(1+x)/2]^{1/2} \tag{32}$$

$$V_m = v_m^1(x)[(1-x)/2]^{1/2} + v_m^2(x)[(1+x)/2]^{1/2}. \tag{33}$$

Now, we consider $W_r^1(h)$ in more detail. Without loss of generality, two spins are

assumed to be located at the zeroth and rth sites. In what follows, three different cases are considered separately.

(i) The impurity is located outside sites between two spins, $h < 0$ or $h > r$. We call this situation 'out'.

(ii) It is located between two spins, $1 < h < r - 1$. We call this situation 'in'.

(iii) The last case, which we call 'on', is the case where an impurity is located at the first or the $(r - 1)$th site.

First let us consider the out case, case (i). For example, when the impurity is located at the $(-h)$th site $(h > 0)$, the spin correlation function is calculated to be

$$W_r^1(-h) = \sum_k \sum_m \frac{B_k}{B_0} E_{km} F_{0m} \left(\frac{\lambda_k}{\lambda_0}\right)^{h-1} y_m^{r-1}. \tag{34}$$

Summing over h, we obtain the contribution from case (i) (the out case) as

$$\sum_{h\in(\text{out})} [W_r^1(h) - W_r^p] = \sum_k{}' \sum_m \frac{B_k}{B_0} \frac{(E_{km}F_{0m} + E_{0m}F_{km})y_m^{r-1}}{1 - \lambda_k/\lambda_0}. \tag{35}$$

Note that we have subtracted the term $k = 0$. (The prime attached to the summation denotes the summation excluding the term $k = 0$.) This expression is valid for $r \geqslant 1$. Secondly, we consider the in case, case (ii), which occurs for $r \geqslant 4$. Defining the integrations, which represent the free-end effect for the correlation,

$$C_m = \int_{-1}^{1} \mathrm{d}x \exp\left(\frac{-x}{2t}\right) V_m(x) \tag{36}$$

$$D_m = \int_{-1}^{1} \mathrm{d}x \exp\left(\frac{-x}{2t}\right) U_m(x) \tag{37}$$

we obtain

$$\sum_{h\in(\text{in})} W_r^1(h) = \frac{L_1(-j/t)}{L_0(-j/t)} \sum_k \sum_m E_{0k} \frac{C_k D_m}{B_0^2} F_{0m} \frac{y_m^{r-3} - y_k^{r-3}}{y_m - y_k}. \tag{38}$$

Lastly, we consider the on case, case (iii). This case, which occurs for $r \geqslant 3$, is very similar to case (ii) and the result is

$$\sum_{h\in(\text{on})} W_r^1(h) = \frac{L_1(-j/t)}{L_0(-j/t)} \sum_m \frac{C_m E_{0m} + D_m F_{0m}}{B_0} y_m^{r-3}. \tag{39}$$

In equations (38) and (39), we see that the spin correlation is finite even when the nonmagnetic impurity is located between two spins as long as J_2 is finite. When $J_2 = 0$, L_1 becomes zero so that there is no correlation as required by consistency.

Summing all contributions up to the linear terms in the concentration x, we obtain the normalised susceptibility χ:

$$\chi t = 1 - x + 2 \sum_r (W_r^p(1 - 2x) + x \sum_h [W_r^1(h) - W_r^p]) + O(x^2)$$

$$= \chi^p t + x\left[-1 + 2\frac{L_1(-j/t)}{L_0(-j/t)}\right.$$

$$\times \left(1 + \sum_m \frac{E_{0m}C_m/B_0}{1-y_m}\right)\left(1 + \sum_m \frac{F_{0m}D_m/B_0}{1-y_m}\right)$$
$$+ 2\sum_k{}' \sum_m \frac{B_k(E_{km}F_{0m} + E_{0m}F_{km})}{B_0(1-\lambda_k/\lambda_0)(1-y_m)}$$
$$- 2\sum_m E_{0m}F_{0m}\frac{(2-y_m)}{(1-y_m)^2}\Bigg] + O(x^2) \tag{40}$$

where χ^p is the susceptibility for the pure case (Harada and Mikeska 1988a). This is our final result for the susceptibility. The numerical results will be presented in graphical form in § 4.

3. Planar chain

Generally speaking, the planar model is similar to the Heisenberg model. For example, the ground state has the same helical spin structure for $j > 0.25$. We note, however, that the difference exists in thermodynamics at low temperatures and has been discussed in connection with the different natures of chiral domain walls in two models (Harada and Mikeska 1988a). Therefore, it is interesting to see how the different effects of non-magnetic impurities are in two models.

For the planar chain, we can apply the transfer matrix method developed in the previous section with some modifications. The partition function for this case is expressed in the same form as equation (13) with a contribution from NNN spins next to an impurity Z_0, which is $I_0(-j/t)$, and a contribution from a chain with n spins Z_n, which is

$$Z_n = \left(\prod_{p=1}^{n}\int_0^{2\pi} \mathrm{d}\theta_p\right)\exp\left(\frac{-(\cos\theta_1 + \cos\theta_{n-1})}{2t}\right)\prod_{p=1}^{n-2} A(\theta_p, \theta_{p+1}) \tag{41}$$

where

$$A(\theta_p, \theta_{p+1}) = \exp\left(\frac{-(\cos\theta_p + \cos\theta_{p+1})}{2t} - \frac{j\cos(\theta_p + \theta_{p+1})}{t}\right). \tag{42}$$

We note that the angle θ_p for $\boldsymbol{S}_p$ is referred to the direction of $\boldsymbol{S}_{p+1}$. This partition function is equivalent to that of the planar chain with NN interactions in a magnetic field. Then, we can evaluate Z_n in a similar way as in the previous section by considering the following integral equation:

$$\int_0^{2\pi} \mathrm{d}\theta_2\, A(\theta_1, \theta_2)\psi_m(\theta_2) = \lambda_m\psi_m(\theta_1) \tag{43}$$

with

$$A(\theta_1, \theta_2) = \exp\left(\frac{-(\cos\theta_1 + \cos\theta_2)}{2t} - \frac{j\cos(\theta_1 + \theta_2)}{t}\right). \tag{44}$$

The result has the same form as equation (9) but B_m should be replaced by

$$B_m = \int_0^{2\pi} \mathrm{d}\theta \exp\left(\frac{-\cos\theta}{2t}\right)\psi_m(\theta). \tag{45}$$

Thus, solving the integral equation (43), we obtain the internal energy and the specific heat for the planar chain.

Correlation functions are also obtained in a similar way, although we need to modify the definitions of some integrals. For the NN and NNN correlation functions, we define B^x_{km} in (20) and B^{xy}_{kg} in (23):

$$B^x_{km} = \int_0^{2\pi} \mathrm{d}\theta\, \psi_k(\theta) \cos\theta\, \psi_m(\theta) \tag{46}$$

$$B^y_{km} = \int_0^{2\pi} \mathrm{d}\theta\, \psi_k(\theta) \sin\theta\, \psi_m(\theta) \tag{47}$$

$$B^{xy}_{kg} = \sum_m (B^x_{km} B^x_{mg} - B^y_{km} B^y_{mg}) \lambda_m. \tag{48}$$

Replacing also L_1/L_0 in (21) by I_1/I_0 we obtained the NN and the NNN correlation functions for the planar model.

The result for the susceptibility (40) is valid if we use the following expressions:

$$E_{km} = F_{km} = \int_0^{2\pi} \mathrm{d}\theta\, \psi_k(\theta) \varphi_m(\theta) \exp\left(\frac{\mathrm{i}\theta}{2}\right) \tag{49}$$

$$C_m = D_m = \int_0^{2\pi} \mathrm{d}\theta\, \varphi_m(\theta) \exp\left(\frac{\mathrm{i}\theta}{2}\right) \tag{50}$$

and

$$y_m = \zeta_m/\lambda_0 \tag{51}$$

where ζ_m and φ_m are the eigenvalue and the eigenfunction of the integral equation:

$$\int_0^{2\pi} \mathrm{d}\theta_2\, A(\theta_1, \theta_2) \exp\left(\frac{\mathrm{i}(\theta_1 + \theta_2)}{2}\right) \varphi_m(\theta_2) = \zeta_m \varphi_m(\theta_1). \tag{52}$$

In the next section, we compare the results with those for the Heisenberg model.

4. Numerical results and discussion

In this section, we present our numerical results which show the characteristic thermodynamic behaviour of the Heisenberg chain and of the planar chain with competing interactions. We have used the 24-point Gaussian integration formula to solve integral equations and to perform integrations. At some points in the parameter space, we have checked the accuracy of our calculation by comparing the result with that obtained by using the 40-point Gaussian integration formula. Another check has been made for the case of $J_2 = 0$ for which we can easily reproduce the exact result. These procedures confirm that, for both models, errors are significant only below $t < 0.05$.

In the numerical calculation, we have adopted the values $j = 0.5$ and $j = 0.2$. The ground state of the former case is helimagnetic while that of the latter case is antiferromagnetic. Furthermore, we fix the concentration at $x = 0.15$ and, for comparison, at $x = 0.0$. The values $j = 0.5$ and $x = 0.15$ may be appropriate for $FeMgBO_4$ (Wiedenmann *et al* 1981).

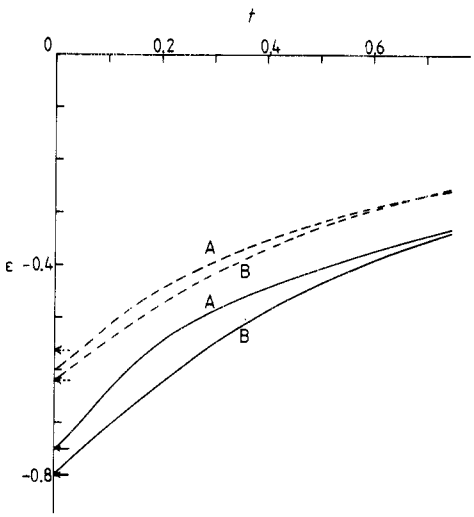

Figure 2. Plots of the internal energy ε per site versus temperature t for the Heisenberg model with $j = 0.5$ (curves A) and $j = 0.2$ (curves B): ---, results for $x = 0.15$; ——, results for $x = 0$; ←, ←---, exact ground-state energies except for the case $j = 0.5$ and $x = 0.15$.

First of all, we show the internal energy ε as a function of temperature t in figure 2 for the Heisenberg model. The results for the planar model are very similar to these and therefore we do not give them here. Before discussing the numerical results, we estimate the ground-state energy for a diluted system. An estimate is easily performed for $j < 0.25$ but it is more subtle for $j > 0.25$. This is because in the former case the ground-state spin structure is antiferromagnetic while in the latter case it is non-trivial. In a first approximation, let us assume that the spin structure is the same as that in the pure case except for an impurity site where two NNN spins couple antiferromagnetically. The result is

$$\varepsilon = W_1 + jW_2 \tag{53}$$

where

$$W_1 = -(1-x)^2/4j \tag{54}$$

$$W_2 = -(1-x)^2[x + (1-x)(1 - 1/8j^2)] \qquad \text{for } j > 0.25 \tag{55}$$

and

$$W_1 = -(1-x)^2 \tag{56}$$

$$W_2 = (1-x)^2(1-2x) \qquad \text{for } 0 < j < 0.25. \tag{57}$$

These values are indicated by the arrows on the ordinate in figure 2 as well as in figures 5 and 6 later. The values for $j = 0.2$ are exact and agree with our calculated result. For $j = 0.5$, however, the helical spin structure changes so as to gain energy by forming a spin complex. This is clearly seen in figure 2 for $j = 0.5$ and $x = 0.15$ as the energy difference between the limiting value and that indicated by the arrow. With temperature increasing from zero, ε increases with a finite slope, which is a consequence of our classical treatment. We see that the steep slope for $j = 0.5$ and $x = 0$ around $t = 0.1$ becomes washed out when the system is diluted with non-magnetic impurities. On the other hand, the result for $j = 0.2$ does not show any significant feature from dilution.

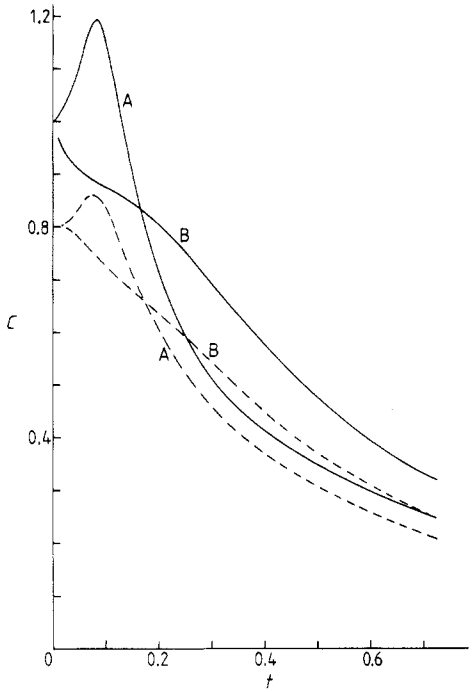

Figure 3. Plots of the specific heat C per site versus temperature t for the Heisenberg model with $j = 0.5$ (curves A) and $j = 0.2$ (curves B): ---, results for $x = 0.15$; ——, results for $x = 0$.

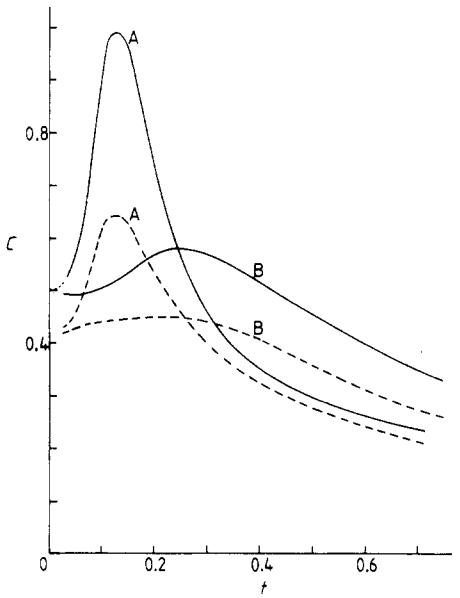

Figure 4. Plots of the specific heat C per site versus temperature t for the planar model with $j = 0.5$ (curves A) and $j = 0.2$ (curves B): ---, results for $x = 0.15$; ——, results for $x = 0$.

This difference is seen more clearly in figures 3 and 4, where the specific heat (which is proportional to the slope of ε) is plotted for the Heisenberg model and for the planar model, respectively, as a function of temperature t. At $t = 0$, C approaches a constant value since our model is classical. In a physical system, the quantum nature of spins manifests itself at low temperatures and hence $C \to 0$ as $t \to 0$. As was discussed in our previous papers (Harada 1984, Harada and Mikeska 1988a) the low-temperature specific heat of a helical chain is dominated by non-linear excitations called the chiral domain wall, whose nature in the Heisenberg model is rather different from that in the planar model. The chiral domain wall in the planar model has Ising character so that the contribution to the specific heat is more pronounced than in the Heisenberg model. When a non-magnetic impurity is introduced in the system, the chirality loses its memory at the impurity site where two NNN spins couple antiferromagnetically without competition. This means that a chiral domain wall is no longer stable topologically. This statement is consistent with the strong reduction in the specific heat of the diluted system for $j = 0.5$. We note, however, that our results for both models cannot be correlated easily to the experimental data of Wiedenmann and Burlet (1978). The reason for this discrepancy is not known at present.

Secondly, the results for the NN and NNN correlation functions W_1 and W_2 as a function of temperature t are shown in figure 5 for the Heisenberg model with $j = 0.5$ and in figure 6 for the planar model with $j = 0.5$. In both cases, we see that, for $x = 0$, W_2 increases very rapidly with decreasing temperature and it reaches a value of -0.5 at $t = 0$. When

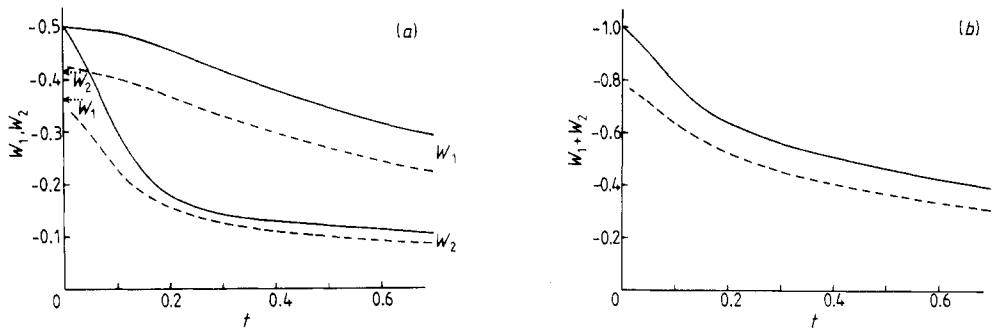

Figure 5. Plots of (*a*) the NN spin correlation function W_1 and the NNN spin correlation function W_2 and (*b*) the sum of the NN and NNN spin correlation functions versus temperature t for the Heisenberg model with $j = 0.5$: ---, results for $x = 0.15$; ——, results for $x = 0$.

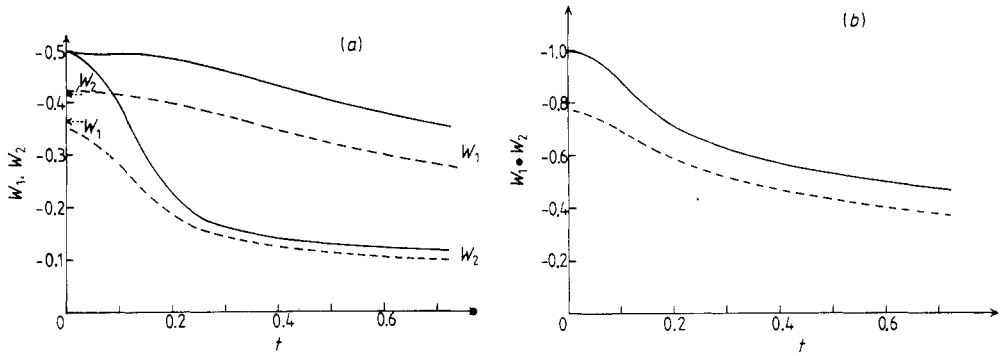

Figure 6. Plots of (*a*) the NN spin correlation function W_1 and the NNN spin correlation function W_2 and (*b*) the sum of the NN and NNN spin correlation functions versus temperature t for the planar model with $j = 0.5$: ---, results for $x = 0.15$; ——, results for $x = 0$.

the system is diluted, W_2 is essentially unchanged at high temperatures but begins to deviate at about $t = 0.2$ and saturates to a significantly smaller value at $t = 0$. This behaviour of W_2 leads to the saturation tendency of the quantity $W_1 + W_2$ which we plot in figures 5(*b*) and 6(*b*). Thus, our calculations reproduce the principal feature of $W_1 + W_2$ observed in $FeMgBO_4$. The quantitative comparison with experimental data, however, is left for a future study on the anisotropic Heisenberg model.

Lastly, we show the susceptibilities χ for the Heisenberg model (in figure 7) and for the planar model (in figure 8) as a function of temperature t. First we note that all susceptibility curves exhibit a rounded maximum at some representative temperature t_0. For the Heisenberg model with $j = 0.5$ it occurs at $t_0 = 0.1$ for the pure case and at a slightly lower temperature for the diluted case. The correction due to non-magnetic impurities is negative for $j = 0.5$ while for $j = 0.2$ it is positive and its magnitude is twice that for $j = 0.5$. In the planar model we see similar features but the magnitude of χ is smaller and the values t_0 are located at rather a high temperature compared with those in the Heisenberg model. The maximum usually disappears in the case of a diluted NN antiferromagnet, since the contribution from the finite chain with odd-number spins

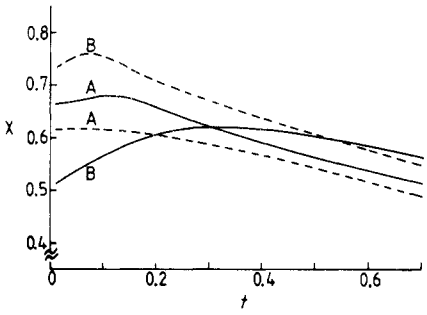

Figure 7. Plots of the susceptibility χ per site versus temperature t for the Heisenberg model with $j = 0.5$ (curves A) and $j = 0.2$ (curves B): ---, results for $x = 0.15$; ——, results for $x = 0$.

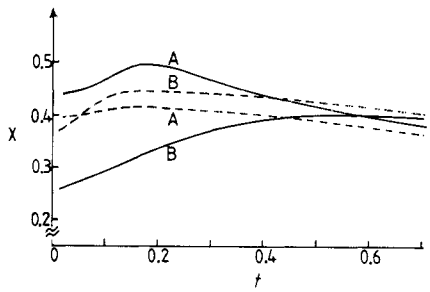

Figure 8. Plots of the susceptibility χ per site versus temperature t for the planar model with $j = 0.5$ (curves A) and $j = 0.2$ (curves B): ---, results for $x = 0.15$; ——, results for $x = 0$.

diverges at low temperatures. In our case, a single non-magnetic impurity breaks the NN interaction but not the NNN interaction so that the correction remains finite even at low temperatures at least for low concentrations. Here we wish to mention that, in diluted systems, the peaks in the χ versus t curves are very broad and the values of t_0 for these peaks are very low compared with the typical energy of the system, e.g. $2J_1$. These features are again consistent with the experimental observations.

5. Conclusion

In this paper, we have developed the transfer matrix method appropriate for a diluted system with NN and NNN exchange interactions. From this method, we have obtained results for the internal energy, the specific heat and the NN and NNN correlation functions, which are exact for an arbitrary concentration of non-magnetic impurities in the sense that we can improve them systematically to any desired degree. On the other hand, our results for the susceptibility are valid up to linear terms in the concentration only.

On the basis of the numerical calculation, we have found that the non-magnetic impurities play characteristic roles especially in the helical short-range order phase for both models. A single non-magnetic impurity breaks up the NN interaction but not the NNN interaction so that two spins next to the impurity couple antiferromagnetically without competition, which means that they form an antiferromagnetic boundary in the helical order. This perturbation spreads over neighbouring spins even at zero temperature. In fact, our calculation for $j = 0.5$ shows that W_1 next to an impurity takes a value closer to -1 than to the bulk value of $-\frac{1}{2}$ (Harada and Mikeska 1988b). Roughly speaking, at low temperatures, the two spins at the NN and second-nearest neighbour positions of an impurity make an angle of $5\pi/6$, and the second- and third-nearest-neighbour spins have already recovered the bulk value of $2\pi/3$. This means that the NN and third-nearest-neighbour spins make an angle of $3\pi/2$, so that W_2 for this spin pair is zero. The tendency of NN spins near an impurity to couple more tightly in an antiferromagnetic manner is in common for all values of j but the length over which the impurity effect spreads depends crucially on j.

These considerations are connected with our numerical results in the following way. Firstly the chiral domain wall is not topologically stable in the diluted system so that the

strong peak in the specific heat versus temperature curve should be reduced. This was observed in figures 3 and 4. Secondly, we discuss the saturation effect of the sum $W_1 + W_2$ which is more significant in the planar model. As has been mentioned above, the larger value of W_1 near impurities yields a more effective energy gain, sacrificing the contribution from W_2. This is clearly seen in figures 5 and 6 where at zero temperature W_1 and W_2 take, respectively, a larger and a smaller value than those estimated by assuming no rearrangement of the spin structure. As a result, W_2 takes a rather small value to keep W_1 large. On the other hand, above the temperature where the magnetic correlation length is shorter than the average distance between impurities, W_2 and W_1 behave as in the pure case. Therefore at some characteristic temperature, which depends on x, W_2 is expected to exhibit the crossover behavior. This is very evident in the case of $j = 0.5$. Although the experimental observations have been made on the sum of W_1 and W_2, we can still recognize the crossover behaviour at low temperatures.

In order to obtain reliable information on the symmetry of the exchange interactions in $FeMgBO_4$, it is probably necessary to perform analogous calculations for the anisotropic Heisenberg chain.

Acknowledgments

This work has been funded by the Bundesministerium für Forschung und Technologie under Contract 03-MI1HAN-6. The numerical calculations were performed at the Regionales Rechenzentrum für Niedersachsen, Hannover.

References

Blume M, Heller P and Lurie N A 1975 *Phys. Rev.* B **11** 4483
Fisher M E 1964 *Am. J. Phys.* **32** 343
Harada I 1984 *J. Phys. Soc. Japan* **53** 1643
Harada I and Mikeska H J 1988a *Z. Phys.* B **72** 391
—— 1988b *J. Physique Coll.* **49** C8 1407
Harada I, Suzuki C and Tonegawa T 1980 *J. Phys. Soc. Japan* **49** 942
Hone D, Montano P A, Tonegawa T and Imry Y 1975 *Phys. Rev.* B **12** 5141
Villain J 1979 *Z. Phys.* B **33** 31
Wiedenmann A 1979 *PhD Thesis* University of Hamburg
Wiedenmann A and Burlet P 1978 *J. Physique Coll.* **39** C8-6 720
Wiedenmann A, Burlet P, Scheuer H and Convert P 1981 *Solid State Commun.* **38** 129
Wiedenmann A, Gunsser W, Burlet P and Mezei F 1983 *J. Magn. Magn. Mater.* **31–4** 1395
Wiedenmann A and Mezei F 1986 *J. Magn. Magn. Mater.* **54–7** 103